Response of the Hyperthermophilic Archaeon *Sulfolobus solfataricus* to UV Damage[▽]†

Sabrina Fröls,[1] Paul M. K. Gordon,[2] Mayi Arcellana Panlilio,[2] Iain G. Duggin,[3] Stephen D. Bell,[3] Christoph W. Sensen,[2]* and Christa Schleper[1]*

University of Bergen, Center for GeoBiology and Department of Biology, Jahnebakken 5, N-5020 Bergen, Norway[1]; University of Calgary, Department of Biochemistry and Molecular Biology, Sun Center of Excellence for Visual Genomics, 3330 Hospital Drive NW, Calgary, AB, Canada T2N 4N1[2]; and MRC Cancer Cell Unit, Hutchison-MRC Research Centre, Hills Road, Cambridge CB20XZ, United Kingdom[3]

In order to characterize the genome-wide transcriptional response of the hyperthermophilic, aerobic crenarchaeote *Sulfolobus solfataricus* to UV damage, we used high-density DNA microarrays which covered 3,368 genetic features encoded on the host genome, as well as the genes of several extrachromosomal genetic elements. While no significant up-regulation of genes potentially involved in direct DNA damage reversal was observed, a specific transcriptional UV response involving 55 genes could be dissected. Although flow cytometry showed only modest perturbation of the cell cycle, strong modulation of the transcript levels of the Cdc6 replication initiator genes was observed. Up-regulation of an operon encoding Mre11 and Rad50 homologs pointed to induction of recombinational repair. Consistent with this, DNA double-strand breaks were observed between 2 and 8 h after UV treatment, possibly resulting from replication fork collapse at damaged DNA sites. The strong transcriptional induction of genes which potentially encode functions for pilus formation suggested that conjugational activity might lead to enhanced exchange of genetic material. In support of this, a statistical microscopic analysis demonstrated that large cell aggregates formed upon UV exposure. Together, this provided supporting evidence to a link between recombinational repair and conjugation events.

Most organisms meet the challenge of maintaining their genome integrity and ensuring correct replication of their genetic material while protecting themselves against the DNA-damaging effects of UV light. This is reflected in the large number of proteins involved in DNA repair pathways, which are found in all three domains of life: *Bacteria*, *Eukarya*, and *Archaea*. For hyperthermophilic organisms, like many archaea, that dwell at the upper temperature limit of life (48), this challenge might be even more demanding. Studies on mutation frequencies and repair in *Archaea* have been inspired by the expectation that extremophiles growing under conditions which accelerate spontaneous DNA damage should be particularly proficient in DNA repair (7, 14, 32). Archaea have also gained special interest because of their unique evolutionary position and their relationship to eukaryotes. Homology in many factors in the systems responsible for transcription and replication has been observed. The homologous, yet simpler, archaeal systems provide a powerful tool for the study of cellular evolution and more complex systems in the eukaryotic nucleus (11). The homology between the eukaryotic and archaeal domains also exists in DNA repair systems (2, 23). For

example, potential factors involved in nucleotide excision repair (NER) of UV-induced DNA lesions are, in most archaea, exclusively constituted by homologs of the eukaryotic proteins XPF/XPB/XPD/Fen-1. The in vivo function of this system in archaea has not yet been elucidated, and the system also seems to be incomplete (23, 39). However, Salerno et al. (42) have shown that *Sulfolobus* can efficiently conduct the repair of photoproducts in the dark, suggesting the presence of an active NER system that is perhaps completed by an as-yet-uncharacterized set of genes. By contrast, in the archaeon *Halobacterium* the bacterial *uvr* system is additionally present, and in that case it seems to be solely responsible for repair of DNA photoproducts in the dark (7).

Notably, some proteins involved in DNA repair systems in bacteria and eukaryotes are absent in most archaea, such as the mutL/mutS mismatch repair machinery (13, 23), indicating that alternative systems might be present (26). Whereas most repair mechanisms act directly on the damaged DNA, unrepaired lesions can also be overcome during replication. A lesion bypass polymerase (Dpo4) (24) has been found in those archaea that contain photolyases, such as the halophiles, which are exposed to strong solar radiation. Some thermophiles from terrestrial hot springs also contain these enzymes (23).

Sulfolobus spp., which reside in solfataras (mud pots) all over the globe, have emerged as important model organisms for biochemical and genetic studies of hyperthermophilic archaea, including analyses of genome integrity and DNA repair. In *S. acidocaldarius* the rate of spontaneous mutation frequencies was found to be comparable to that of other microorganisms, indicating that hyperthermophiles are able to maintain

genomic stability, despite the extreme growth conditions (15). The anaerobic hyperthermophilic euryarchaeote *Pyrococcus furiosus* has an astonishingly high resistance to gamma irradiation and a highly efficient repair mechanism for double-strand DNA breaks (DSB) (36, 51); by contrast, the sensitivity of *S. acidocaldarius* to gamma irradiation was found to be comparable to that of *Escherichia coli* (33). Similarly, mutational analyses after exposure to short-wavelength UV light revealed that *Sulfolobus* was as sensitive and equally UV mutable as *E. coli* and exhibited effective photoreactivation under visible light (52). In line with these findings, Salerno et al. (42) identified *cis*-syn-cyclobutane pyrimidine dimers (CPDs) in *Sulfolobus solfataricus* after treatment with UV light, which together with pyrimidine 6-4 pyrimidone photoproducts (6-4PP), are known to be direct consequences of UV-induced damage. The same authors demonstrated repair of CPDs in the dark, suggesting the presence of an active NER pathway in *Sulfolobus* (42). However, unlike in other organisms, in *Sulfolobus* it seems to act with the same efficiency on both DNA strands, lacking a transcription-coupled activity (8, 39). Interestingly, an increased rate of exchange of genetic markers was observed with *S. acidocaldarius* mutants upon treatment with UV light, and it was hypothesized that DNA lesions and double-strand breaks stimulate this process (47, 52).

Sulfolobus solfataricus is a host for the virus SSV1, which contains a 15.5-kb double-stranded circular DNA genome that site specifically integrates into the host chromosome. Viral replication and propagation are strongly inducible by UV light (27, 35, 45), which led to the early speculation that *Archaea* might have an SOS-like system (27). Two recent genome-wide transcriptional studies in *Halobacterium* sp., however, did not reveal a concerted induction of the genes involved in excision repair or other damage reversal genes (3, 29). Instead, only genes involved in homologous recombination seemed to be induced when cells were exposed to low doses of UV light (30).

Here we describe a genome-wide transcriptional analysis of the response of *Sulfolobus solfataricus* to UV irradiation that was designed to investigate the general UV response of a hyperthermophilic archaeon. Our studies are complemented by analyses of double-strand break formation, the cell cycle, and cell physiology.

MATERIALS AND METHODS

Growth of *Sulfolobus* strains and UV treatment. *S. solfataricus* strains PH1 (46) and PH1(SSV1) (28) were grown at 78°C and pH 3 in Brock's medium (12) with 0.1% (wt/vol) tryptone and 0.2% (wt/vol) D-arabinose under moderate agitation (ca. 150 rpm in a New Brunswick shaker). The optical density of liquid cultures was monitored at 600 nm. For survival rate and UV dose determinations, solid media were prepared by adding gelrite to a final concentration of 0.6% and Mg^{2+} and Ca^{2+} to 0.3 and 0.1 M, respectively. Plates were incubated for 5 days at 78°C. For UV treatment, aliquots of 50 ml (optical density at 600 nm, 0.3 to 0.5) were transferred to a plastic container (20 cm by 10 cm by 4 cm) and irradiated with UV light for 45 s at 245 nm (W20; Min UVIS; Degesa) while shaking the culture carefully. The treated cultures were stored in the dark at room temperature for 15 min and were reincubated at 78°C.

Survival rate of *S. solfataricus* after different UV doses. The plating efficiency (CFU/ml) of *S. solfataricus* cells after treatment with different UV doses (UV-C, 254 nm) was determined using a logarithmically grown culture (Brock's basal salt medium with 0.1% [wt/vol] tryptone and 0.2% [wt/vol] D-arabinose). For the UV treatment, 10 ml of culture was transferred to a 110-mm plastic petri dish and treated with a defined UV dose of 200 J/m², 150 J/m², 100 J/m², 75 J/m², 50 J/m², or 25 J/m² (λ, 254 nm; UV-Stratalinker 1800; Stratagene). Additionally, two independent treatments were performed with a UV lamp (W20; Min UVIS;

Degesa, Heidelberg, Germany) for 45 s at 254 nm. All treatments were performed under red light. For the control culture, exactly the same procedure was followed under red light (incubation, 45 s) without UV treatment. The treated cultures were stored in the dark at room temperature for 15 min and were subsequently plated (dilutions of 10^{-4}, 10^{-5}, and 10^{-6}). Plates were incubated for 5 days at 78°C. Numbers of CFU per ml were determined, and the survival rate (percentage) was calculated.

Microscopy and analysis of cell aggregate formation. Cell aggregates were analyzed with a phase-contrast microscope (Axioskop; Zeiss) with ×1,000 magnification. To fix the cells, microscope slides were coated with solid medium. One ml of twofold-concentrated Brock salt solution (12) with 2% $MgCl_2$, pH 3, without carbon sources was preheated to 78°C and mixed with 1 ml of melted 1.3% gelrite (Merck and Co. Kelco Division) in distilled 78°C water. A 500-μl aliquot of the solution was immediately poured on a microscope slide, and a coverslip was added. After about 1 min, the coverslip was removed. Then, 5 μl of pure *S. solfataricus* culture or culture diluted 1:2 with 1× Brock salt solution, pH 3, 78°C, was added, and a coverslip was placed on top before microscopy was performed. To quantify the formation of aggregates, the cells in aggregates were counted until 1,000 or 500 single cells were observed, respectively. For the statistical analysis, the percentage of cells in aggregates versus the single cells was calculated from three independent experiments. The images were digitized with a microscope-coupled-device camera (Power Shot G6; Canon) connected to a computerized image analysis system (Remote Capture; Canon Utilities). To analyze the cell vitality, the Live/Dead *Bac*Light (Invitrogen) assay was used.

Fluorescence-activated cell sorter analysis. Cells were fixed by addition to ice-cold 80% ethanol (70% ethanol, final concentration). For staining, cells were washed two times with 10 mM Tris-HCl (pH 7.4), 10 mM $MgCl_2$ and then resuspended in this buffer containing an additional 20 $\mu g \cdot ml^{-1}$ propidium iodide and 100 $\mu g \cdot ml^{-1}$ RNase A. Fluorescence-activated cell sorter cytometric analysis was carried out using a MoFlo high-speed cell sorter (Dako Cytomation) as described previously (37).

Analysis of chromosomal DNA by PFGE. To identify DSB in DNA, cells were embedded in agarose plugs before cell lysis was performed. A 15-ml volume of the cell culture was harvested for approximately three plugs. Cells were washed twice with 10 ml TEN solution (50 mM Tris-Cl, pH 8; 50 mM EDTA, pH 8; 100 mM NaCl) and centrifuged at 4,000 rpm for 10 min at 4°C between each washing step. Washed cells were finally resuspended in 100 μl TEN solution. The cell solution was briefly warmed to 37°C and then immediately mixed with 100 μl of 0.8% low-melting-point agarose (precooled to 37°C). An 85-μl aliquot of the agarose cell solution was dispensed into wells of a disposable plug mold (catalog no. 1703706; Bio-Rad) and incubated for 15 min at 4°C. Congealed plugs were transferred to a 2-ml tube containing 2 ml of NDS solution (0.5 M EDTA, 0.12% Tris, 0.55 M NaOH, pH 9.0) and 1 mg/ml proteinase K and incubated overnight at 37°C. The liquid was replaced with 2 ml NDS, pH 8.0, with 1 mg/ml proteinase K added and incubated again overnight at 37°C. Plugs were then washed with 2 ml NDS, pH 8.0, and stored in 2 ml of NDS, pH 8.0, at 4°C. For pulsed-field gel electrophoresis (PFGE), we used a CHEF-DR III pulsed-field electrophoresis system (Bio-Rad) with a permanent circulation of 0.5× Tris-borate-EDTA buffer. Electrophoresis was run for 20 h at 6 V/cm (increasing the pulse time from 5 to 50 s) at 14°C. The PFGE gel was stained for 10 min with SYBR Green (1:100,000 in 1× Tris-borate-EDTA; Fluka), and the image was created with a PhosphorImager (FLA-5000; Fujifilm).

RNA preparation and analysis. Total RNA was extracted using a standard procedure (5). RNA quality was determined by agarose gel electrophoresis and by determination of the ratio of absorption at 260 nm and 280 nm. Only RNA samples with a ratio between 2.1 and 1.9 were used for further experiments.

Microarray design and fabrication. Each microarray consisted of 3,456 70-mer oligonucleotides spotted onto glass slides. The design and fabrication methodologies for the microarrays were the same as those described in detail in another recent study (9).

cDNA labeling and microarray hybridization. Labeling of cDNA and microarray hybridizations with cyanine-3 or cyanine-5 (Cy-3/Cy-5) fluorescent molecules were performed as described recently (9). Each slide hybridization experiment was repeated as a dye swap, and each time point was analyzed by combining results of hybridizations from four independent UV experiments. This resulted in a total of 6 to 12 data points for each gene at each time point as the basis for the quantitative and statistical analysis. In total, 62 successful hybridizations were performed in order to obtain the 8.5-h time series.

Microarray data analysis. Qualitative and statistical analyses of the data were performed as recently described (9). A K-means clustering (KMC) analysis was performed using the TIGR MultiExpressionViewer (41) integrated into the program Bluejay (50) (see Fig. S2 in the supplemental material). The K-means were calculated from the genomic microarray data set of the virus-infected

TABLE 1. Survival fraction of *S. solfataricus* cells after treatment with UV light

UV dose (J/m^2)	Survival of *S. solfataricus* after UV treatment[a]		Survival fraction (%)[b]
	CFU/ml (absolute)	SD	
0	2.41×10^8	1.40×10^8	100
25	1.35×10^8	9.43×10^7	56
50	9.40×10^7	5.17×10^7	40
75	2.47×10^7	1.07×10^7	11
100	5.81×10^6	3.10×10^6	2.5
150	5.33×10^4	4.11×10^4	0.03
200	6.67×10^3	9.43×10^3	0.0003

[a] An exponentially grown culture was treated with different UV doses from 25 J/m^2 to 200 J/m^2, and CFU/ml were determined after plating of the cells. Means and standard deviations of three replicates are given.
[b] Relative to CFU at 0 J/m^2.

PH1(SSV1) and the noninfected PH1 strains. The genes were sorted into 40 clusters with a maximum of 50 iterations. To identify the main genomic UV answer, we focused our analysis on genes which showed a significant change in the expression rate over the time course. The KMC analysis identified the same genes as we identified by manual analysis for both tested strains. Besides the KMC analysis, we surveyed the genomic microarray data for specific gene groups of main cellular events, such as cell cycle, replication, transcription, translation, and repair, based on COG categories (Clusters of Orthologous Groups of proteins [http://www.ncbi.nlm.nih.gov]). The PH1 and PH1(SSV1) data sets are available at the Bluejay website for *Sulfolobus* (http://bluejay.ucalgary.ca/sulfolobus).

RESULTS

Survival and growth of *S. solfataricus* cells after exposure to UV light. To evaluate the impact of UV irradiation on *S. solfataricus*, we first analyzed cell viability after UV doses in a range from 25 to 200 J/m^2 of UV-C (254 nm) (Table 1). The UV dose of 75 J/m^2, which was used in all further experiments, yielded a plating efficiency of approximately 10 to 40% compared to nontreated cells. Figure 1 displays representative growth rates of UV-irradiated (75 J/m^2) and control cultures of *S. solfataricus* PH1. The strain showed a growth retardation after UV treatment compared to the mock-treated control culture.

UV exposure induces formation of cell aggregates. Microscopic examination of cells revealed the formation of cell aggregates between 3 and 10 h after UV treatment, with the greatest level of aggregation appearing on average 6 h after the UV treatment (Fig. 2). On average, two to five cells were found in the early aggregates, while bigger complexes tended to form later. The formation of cell aggregates was similar in both strains, i.e., was independent of the virus SSV1, and was highly reminiscent of the formation of aggregates observed in the context of plasmid-mediated conjugation (44). We saw much less or even no aggregate formation at all when the cells were exposed to higher doses of UV light (200 J/m^2), indicating that the cell clumping did not represent a nonspecific aggregation of dead cells (not shown). Furthermore, differential staining (see Materials and Methods) indicated that at least 50% of the cells within the aggregates were metabolically active (data not shown). We therefore conclude that the aggregation of the cells most probably represents a regulated cellular reaction to the UV treatment.

Analysis of cellular DNA content by flow cytometry. During exponential growth, *Sulfolobus* cells remain in the G_2/M phase of the cell cycle for a relatively long time period, with only a very short G_1 phase (20). Therefore, most cells of an unsynchronized, exponentially growing *Sulfolobus* culture contain two genomes, while a considerably smaller fraction contains only one. Figure 3 shows the DNA content distribution of an exponential culture of *S. solfataricus* PH1, acquired by flow cytometry (Fig. 3, left row, control). After UV treatment of an exponential culture, we observed an initial modest accumulation of cells with DNA contents that coincided with cells in the G_1 and S phases of the normal cell cycle (Fig. 3, 0.5 h to 5 h of UV treatment). Five hours after the UV treatment, this effect became more obvious, and in addition, a heterogeneous population of cells containing greater than two chromosome equivalents became apparent, which was most obvious after 8.5 h post-UV treatment. A similar phenotype has been observed after treatment of *S. solfataricus* with hydroxyurea, a likely DNA-damaging agent (I. G. Duggin and S. D. Bell, unpublished data). Similar data to those shown in Fig. 3 were obtained with the PH1(SSV1) strain (see Fig. S1 in the supplemental material).

Formation of double-strand breaks. While CPDs have been demonstrated to occur in *Sulfolobus* after UV treatment (42), it has not been investigated if DSB are formed as a result of unrepaired lesions during replication, similar to those observed in *E. coli* (4) and yeast (16) and more recently described in mouse cells (10). In order to analyze the formation and extent of double-strand breaks, we analyzed DNA prepared after UV treatment using pulsed-field gel electrophoresis (Fig. 4). A considerable accumulation of chromosomal fragments of smaller sizes than in the control samples was observed, peaking at 2 h after UV treatment but visible until 8 to 10 h after UV treatment. The most abundant fraction of fragments captured in this analysis ranged from 100 kb up to 600 kb in size, mostly because the electrophoresis conditions were chosen such that all fragments of 600 kb and bigger were compressed in the upper part of the gel. No DSB were observed at time zero (cells harvested immediately after treatment; this might indicate that their formation was not a direct result of the UV
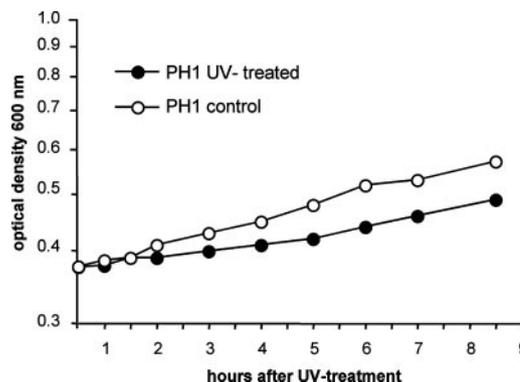

FIG. 1. Representative growth curve of *S. solfataricus* PH1 after UV treatment. A UV dose of approximately 75 J/m^2 (254 nm) was used for the treatment, and the cultures were recultivated at time point 0 h. The time points of sampling for DNA and RNA extractions are indicated by the symbols.
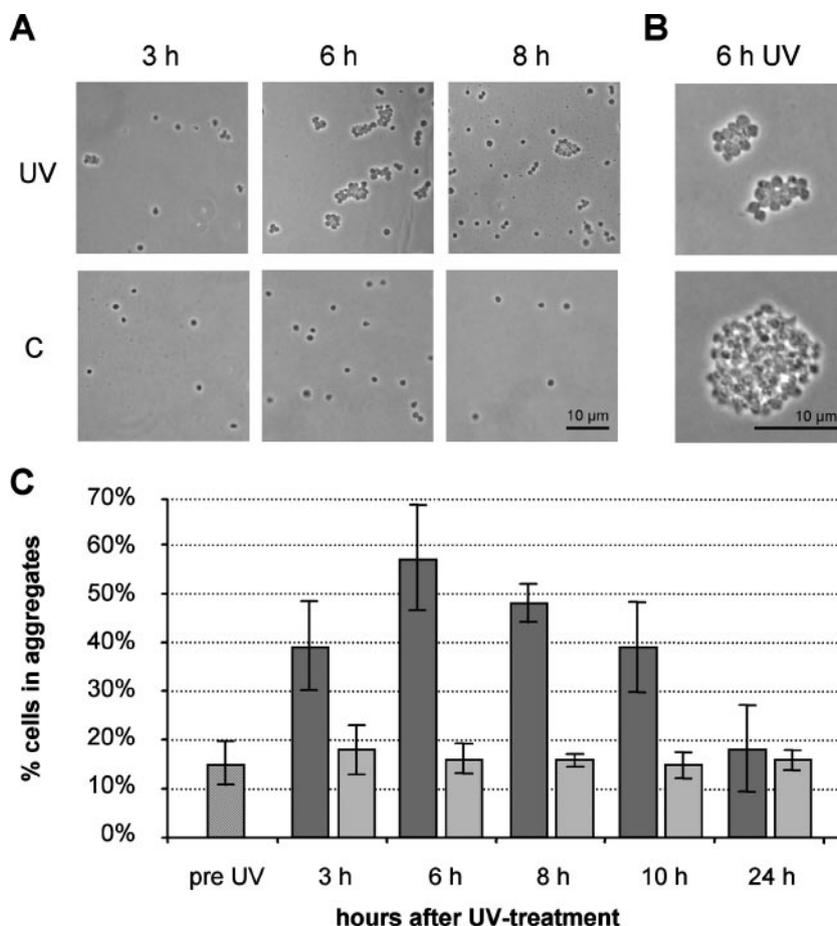
FIG. 2. Aggregation of *S. solfataricus* cells after UV treatment. (A) Micrographs (phase contrast) of *S. solfataricus* cells fixed on a gelrite-coated microscope slide. Representative pictures of cells and/or aggregates at 3 h, 6 h, and 8 h after UV treatment are shown. C, control culture without UV treatment. An increasing amount of cell aggregates was observed in UV-treated cultures after 3 h. (B) Top: typical cell aggregates, as observed around 3 to 6 h after UV treatment. Bottom: typical maximum cell aggregate, mostly discovered at 6 h after UV treatment; these data are excluded from the results shown in panel C, because the number of cells was uncountable. (C) Quantitative analysis of cell aggregate formation at different time points after UV treatment. The pre-UV culture was split into a UV-treated culture (dark gray) and a control culture (light gray). The amount of cells in and out of aggregates was counted until 1,000 single cells were found in total. Means and standard deviations (error bars) are shown from three independent UV experiments. The amount of cells found in aggregates is an underestimate, because cells in the large aggregates were not countable (see panel B description in the legend).

treatment per se but, rather, a result of subsequent cellular processes). However, less material seemed to have been separated in those lanes.

By contrast, we observed CPD formation at time zero (data not shown), consistent with previous findings (42), suggesting that CPDs are a direct result of the UV treatment.

General transcriptional response. For each of the four independent UV time series experiments, RNA was isolated from UV-treated and control cells and analyzed using Northern hybridization to evaluate the quality of the isolated nucleic acids and to verify induction of the viral cycle in the lysogenic PH1(SSV1) strain (9) as well as of some UV-responsive chromosomal genes (not shown). For microarray hybridizations, the total RNA was reverse transcribed and dual labeled with fluorescent dyes. We identified 55 UV-responsive genes in *S. solfataricus* that exhibited a pronounced change in mRNA copy numbers over an extended period of time. Among these were 19 genes that we categorized as being strongly induced genes based on KMC analysis (Table 2, group Ia; see also Fig. S2 in

the supplemental material). Another 14 genes showed a similar expression pattern as group Ia but had smaller amplitudes in mRNA level changes in the KMC analysis (Table 2, group Ib). A third group of 22 genes represented the most pronounced down-regulated genes (group II). The average expression profiles of these groups are presented in Fig. 5 (see also Fig. S3 in the supplemental material; single ratios are listed in Tables S1 and S2 of the supplemental material). The figure shows that the UV-dependent response over time lasted from ca. 1.5 h after UV treatment until 5 h. The start of the transcriptional response in the lysogenic strain PH1(SSV1) was observed considerably earlier and the response was generally stronger, with an average maximal induction level of group Ia genes of 12-fold ($\log_2$ of 3.5) versus 6-fold ($\log_2$ of 2.5) for strain PH1 (see Fig. S3 in the supplemental material). Therefore, the use and comparison of data from both strains helped in dissecting those genes that showed a significant UV-dependent response. Immediately after the UV treatment, a large number of genes seemed to be induced over only a short time period (1 to 1.5 h
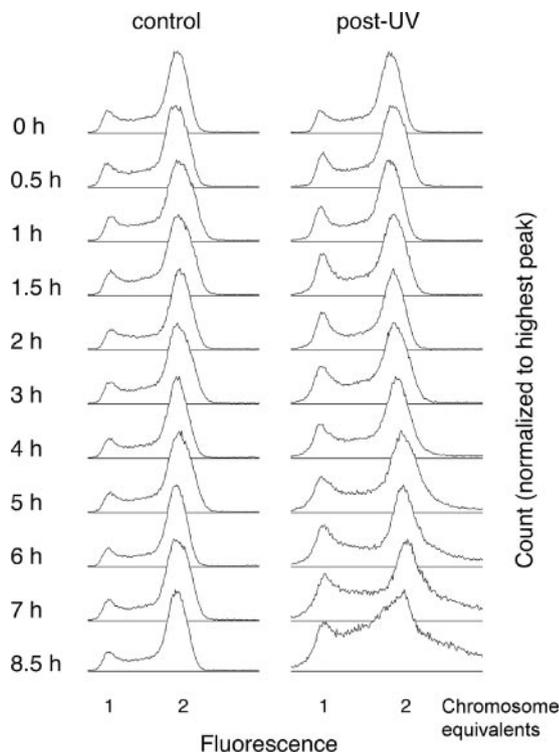
FIG. 3. Flow cytometry analysis of *S. solfataricus* cells after UV treatment (strain PH1). Cells were fixed in 80% ice-cold ethanol, and the DNA contents were measured by fluorescence [see Fig. S1 for data for strain PH1(SSV1)]. Samples from the UV-treated culture (post-UV) and the mock-treated control culture (control) were analyzed from 0 h to 8.5 h. A chromosome content of 1N ("1" on the *x* axis) is found in G_1 phase, between 1N and 2N represents S phase (DNA synthesis), and 2N is the G_2 phase of the cell cycle (20).
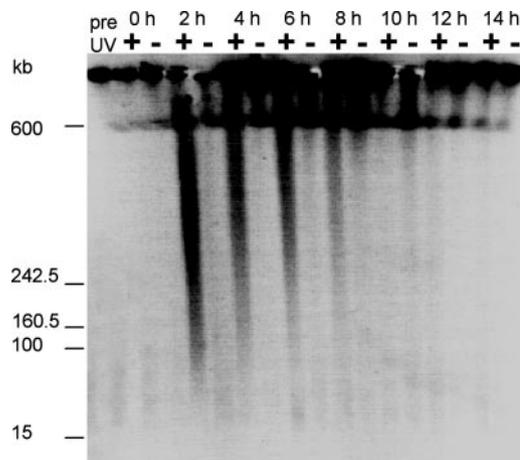

FIG. 4. PFGE analysis of total DNA from *S. solfataricus* PH1 after UV treatment to determine the extent of DSB. DNA from UV-treated (+) and control (-) cells was analyzed from 0 h to 14 h after UV treatment and pre-UV. Fragmentation of DNA is visible as a smear in the area of the gel below the compression zone (at 600 kb), from 2 h to 8 h, mostly in the UV-treated samples.

after UV) in strain PH1 and to a lower extent in the infected PH1(SSV1) strain (Fig. 5). They mostly encode factors involved in translation and transcription, as well as housekeeping proteins involved in central metabolic pathways or information processing. A significant increase ($P < 0.05$ in three experimental replicates) in the mRNA levels of these approximately 400 genes in strain PH1 was found immediately after UV treatment until 1.5 h after. This spike occurred before and is distinct from the long-duration regulation (up or down) of genes in the 1.5-to-7-h range (Fig. 5). We postulate that the genes which show a significant change in mRNA levels over this very short time period appear up-regulated because (i) they are strongly transcribed genes and (ii) the cell cycle was modestly perturbed due to the UV treatment. In order to get insights into the effect of UV treatment on central processes within the cell, we looked into the data sets for all genes involved in information processing (e.g., replication, transcription, and translation, based on COGs). We found that most of these genes followed the general expression pattern (Fig. 5), although not all peaked considerably (>2- or <−2-fold change).

Differential reaction of the three *cdc6* genes in *Sulfolobus*. One of the most pronounced transcriptional reactions after UV treatment was a rise in the mRNA level of the *cdc6-2* gene

in both *Sulfolobus* strains and a down-regulation of *cdc6-1*, while the *cdc6-3* gene remained essentially unaffected (Fig. 6).

The *cdc6-2* gene was found to be cotranscribed with two other strongly induced open reading frames, one of which encoded a hypothetical transcription regulator that could play a role in UV-effected transcriptional responses and the second representing a *moaC* gene, an accessory protein for molybdenum cofactor biosynthesis (18) (see Fig. S4II in the supplemental material).

The UV-induced transcriptional response in *S. solfataricus* is limited to 55 genes. Besides the *cdc6-2* operon, we found a further 30 up-regulated genes that reacted most strongly upon UV treatment (Table 2, groups Ia and Ib), 13 of which are organized in operons (Table 2, column 7). Among these was a large group of genes encoding hypothetical membrane proteins or proteins with signal peptides, like the two strongly up-regulated genes SSO691 and SSO3146. One operon encoded homologs of a putative type II/IV secretion and/or type IV pilus system (Fig. 7), with an ATPase (SSO0120), a putative transmembrane protein (SSO0119), and two small proteins (SSO118 and SSO117) with a type IV pilin-like signal peptide (1). SSO0120, when compared to hidden Markov models of NCBI's COG database (unpublished), was identified as an ATPase involved in archaeal flagellar biosynthesis and also matches the central domain of the Flp pilus assembly protein. Also supported by the context of other observations, this operon is likely involved in the synthesis of conjugation pili (see Discussion, below), instead of encoding a secretion system. Other strongly induced genes encode potential transcription factors (SSO0280 and lam04_n0008), which could be involved in regulating the UV-induced transcriptional response, and two genes encoding AAA$^+$ ATPases (SSO0152 and SSO0283). Genes putatively involved in DNA repair processes are discussed in a separate paragraph below.

In group Ia, which contains the highest induced genes, we found also the immediate early transcript T-ind of SSV1 in

TABLE 2. UV-dependent regulated genes of *S. solfataricus*

Group[a]	Induction or repression in strain[b]:		Gene[c]		COG no.	Operon[d]	Predicted function[e]	Homology[f]
	PH1	PH1(SSV1)	Name	ID				
Ia	HI	HI		SSO0691			Conserved hypothetical membrane protein, 7 TMD, N-terminal SP	C
	HI	HI		SSO0280	1405K		Conserved hypothetical, potential transcription factor	C
	HI	HI		SSO3146			Conserved hypothetical membrane protein, 7 TMD, N-terminal SP	C
	HI	HI		SSO1501			Conserved hypothetical	C
	HI	HI	*cdc6-2*	SSO0771	1474L	1 (1/3)	Cell division control protein, same operon order in *S. acidocaldarius* and *S. tokodaii*	A, E
	HI	HI		c54_n0003_1		2 (1/2)	Hypothetical	
	HI	HI	*gspE-1*	SSO0120	0630N	3 (2/5)	Putative ATPase of typeII/IV secretion system protein	A, B
	HI	HI		SSO0152	0433R		Conserved hypothetical (VirD4-like ATPase)	S
	HI	HI		SSO2338	0477G		Conserved hypothetical transport protein, 5 TMD	A
	HI	HI	*dpo2* AT	SSO8124		4 (1/3)	DNA polymerase B2 amino end, same operon order in *S. acidocaldarius* and *S. tokodaii*	S
	HI	HI		SSO0283	0433R		Conserved hypothetical probable ATPase, N-terminal SP	S
	HI	HI		SSO0117		3 (5/5)	Conserved hypothetical, with pilin-like SP	S
	HI	HI		SSO0118		3 (4/5)	Conserved hypothetical, with pilin-like SP	S
	HI	HI		SSO1053			Conserved hypothetical, N-terminal SP	S
	HI	HI		SSO0037			Hypothetical, N-terminal SP	
	HI	HI		SSO2395			Conserved hypothetical	S
	I	HI		SSO1458		4 (3/3)	Conserved hypothetical	C
	HI	HI	*dpo2* CT	SSO1459	0417L	4 (2/3)	DNA polymerase B2 carboxy end	A
	HI	HI	*insB*	SSO1436	1662L		Transposase and inactivated derivatives, IS*1* family	S
				SSO1654	1662L		Transposase and inactivated derivatives, IS*1* family	
				SSO2320	1662L		Transposase and inactivated derivatives, IS*1* family	
				SSO2950	1662L		Transposase and inactivated derivatives, IS*1* family	
Ib	I	I		SSO0001	1468L		Conserved hypothetical nuclease, RecB family	A
	I	I		SSO3177			Conserved hypothetical, N-terminal SP	S
	I	I	*herA*	SSO2251	0433R	5 (1/4)	3′–5′ ssDNA helicase, same operon order in *S. acidocaldarius* and *S. tokodaii*	A, B
	I	I		c43_n0005			Hypothetical	
	SI	I	*bcp-2*	SSO2121	0450O		Peroxiredoxin	A, B, E
	SI	I		SSO0823			Conserved hypothetical	S
	I	I	*moaC*	SSO0770	0315H	1 (3/3)	Molybdenum cofactor biosynthesis C	A, B, E
	I	I		SSO1823			Conserved hypothetical	S
	I	I		c44_n0017			Hypothetical	
	I	I		bac03_n0001			Hypothetical	
	I	I		lam04_n0008		1 (2/3)	Conserved hypothetical transcription regulator	C
	I	I		bac18_n0006			Hypothetical	
	HI	I		SSO0121		3 (1/5)	Conserved hypothetical, same operon order in *S. acidocaldarius* and *S. tokodaii*	S
	I	I		SSO0119	2064N	3 (3/5)	Conserved hypothetical membrane protein, 9 TMD, N-terminal SP	S

Continued on following page

TABLE 2—Continued

Group[a]	Induction or repression in strain[b]:		Gene[c]		COG no.	Operon[d]	Predicted function[e]	Homology[f]
	PH1	PH1(SSV1)	Name	ID				
II	R	R		SSO0909	0464O	7 (3/3)	Conserved archaeal AAA$^+$ ATPase	A, B, E
	R	R		SSO2288	0477G		Conserved hypothetical membrane protein, 9 TMD and N-terminal SP	S
	R	R		SSO3242	1321K		Conserved hypothetical transcriptional regulator	S
	SR	R		SSO2750		8 (2/2)	Conserved hypothetical (ATPase), same operon order in *S. acidocaldarius* and *S. tokodaii*	S
	SR	R		SSO2751		8 (1/2)	Conserved hypothetical kinase	S
	SR	R	cdc6-1	SSO0257	1474L		Cell division control 6/orc1 protein homolog	A, E
	SR	R	soj	SSO0034	1192D		Conserved ATPases involved in chromosome partitioning	A, B
	R	R		SSO0910	5491N	7 (2/3)	Conserved hypothetical, VPS24 domain	C
	R	R		SSO0881	5491N		Conserved hypothetical, VPS24 domain	C
	SR	R		SSO0858		9 (2/2)	Conserved hypothetical	C
	R	R		SSO5826	3609K		Conserved protein, potential transcription regulator	A
	SR	R		SSO6687		9 (1/2)	Conserved hypothetical, same operon order in *S. acidocaldarius* and *S. tokodaii*	S
	R	R		SSO10704			Conserved hypothetical	A
	SR	R		SSO3207			Conserved hypothetical kinase	S
	R	R		SSO0451	5491N		Conserved hypothetical, VPS24 domain	C
	SR	R		SSO2200	0433R		Conserved hypothetical probable ATPase	A, B
	R	R		SSO0911		7 (1/3)	Conserved hypothetical, same operon order in *S. acidocaldarius* and *S. tokodaii*	C
	R	SR		SSO3066	1653G		Arabinose-binding protein, ABC transporter	A, B
	R	SR	ssh7A	SSO9180			7-kDa DNA-binding protein (Sso7d-2)	S
	R	SR	ssh7A	SSO10610			7-kDa DNA-binding protein (Sso7d-1)	S
	R	SR	ssh7A	SSO9535			7-kDa DNA-binding protein (Sso7d-3)	S
	R	SR		SSO0271	1222O		26S proteasome regulatory subunit	A, E

[a] UV-dependent regulated gene groups were identified by a KMC analysis (see also Fig. S2 in the supplemental material). Ia, highly induced gene group; Ib, induced gene group; II, repressed gene group.

[b] HI, highly induced; I, induced; SI, slightly induced; SR, slightly repressed; R, repressed.

[c] Genes without an SSO number are intergenic small open reading frames of less than 300 nucleotides.

[d] Number of the operon (1 to 9) and, in parentheses, the position in the operon and total number of genes in the operon.

[e] TMD, transmembrane domain; SP, signal peptide; ssDNA, single-stranded DNA.

[f] Homologs (BLASTP E-values $< 10^{-40}$). S, *Sulfolobaceae*; C, *Crenarchaeota*; A, *Archaea*; B, *Bacteria*; E, *Eukarya*.
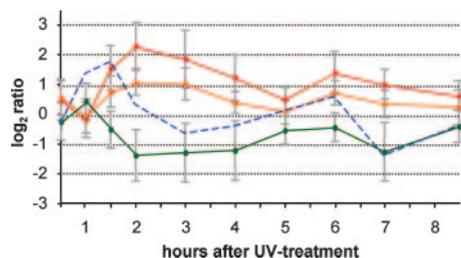

FIG. 5. Expression profiles of the general transcriptional response after UV treatment of strain PH1. The curves display the means of the three identified UV-dependent regulated gene groups as displayed in Table 2: the highly induced group of 19 genes (red curve), the induced gene group of 14 genes (orange), and the down-regulated group of 22 genes (green). The blue dashed curve was generated from the averages of 11 genes but represents qualitatively the pattern of approximately 400 gene that are mostly involved in the transcription and translation processes. Errors bars do not represent standard deviations but express the range of gene expression of the different genes that are "summarized" in each line.

strain PH1(SSV1), which can be considered a positive control in this data set, as its UV dependence and transcriptional pattern have been well characterized (9, 35).

Among the 22 prominent down-regulated genes (including three operons), we found some encoding potential regulators (SSO3242 and SSO5826), kinases (SSO2751 and SSO3207), transporters (SSO2288 and SSO3066), and diverse ATPases (SSO0909, SSO2750, and SSO2200). Among the last group is the Soj protein, which may be involved in chromosome segregation. Three genes, which can also be found in other crenarchaeota (SSO0910, SSO0881, and SSO0451), have a conserved VPS24/SNF7 domain, which in eukaryotes is involved in the transport of cellular or transmembrane proteins between the endosomes and lysosomes for degradation events (19). Of these, SSO0910 belongs to an operon with three genes (operon 7) (see Fig. S4I in the supplemental material) that shows the
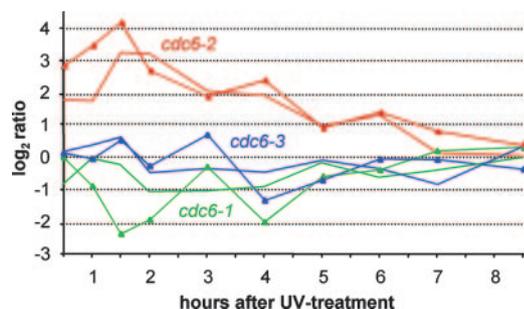
FIG. 6. Expression profiles of the three *cdc6* genes in both strains PH1 (sleek lines) and PH1(SSV1) (lines with triangles) showed a strong up-regulation of the potential repressor of replication *cdc6-2* (red), shortly after UV treatment, while the potential main initiator of replication *cdc6-1* (green) is repressed. The data represent means of two to three experiments, but the display of standard deviations has been omitted for clarity.

strongest down-regulation after UV treatment (SSO0911, SSO0910, and SSO0909).

Interestingly, the three genes for SSO7d, encoding one of the two types of chromatin proteins in *Sulfolobus* (SSO10610, -9535, and -9180), are also down-regulated.

Proteins potentially involved in repair of DNA damage. All genes potentially involved in repair systems that have been specifically inspected with respect to their UV response are listed in Table S3 of the supplemental material. Almost none of the genes supposedly involved in damage reversal, including

FIG. 8. Expression profile of the archaeal *rad50/mre11* operon after UV treatment. The transcriptional activity was first detected in *S. acidocaldarius*. *herA*, archaeal *he*licase, encodes a new class of bipolar DNA helicases (6); *mre11*, single-stranded DNA endonuclease and 3′-to-5′ double-stranded DNA exonuclease; *rad50*, ATPase; *nurA*, *nu*clease of *a*rchaea, a 5′-to-3′ exonuclease. The four genes, which are supposedly involved in homologous recombination as part of the putative recombination repair system, show a weak but significant UV-dependent response, while *radA* (SSO0250; blue curve) follows the pattern of highly transcribed genes (see the blue line in Fig. 5, above). (A) Strain PH1; (B) strain PH1(SSV1).
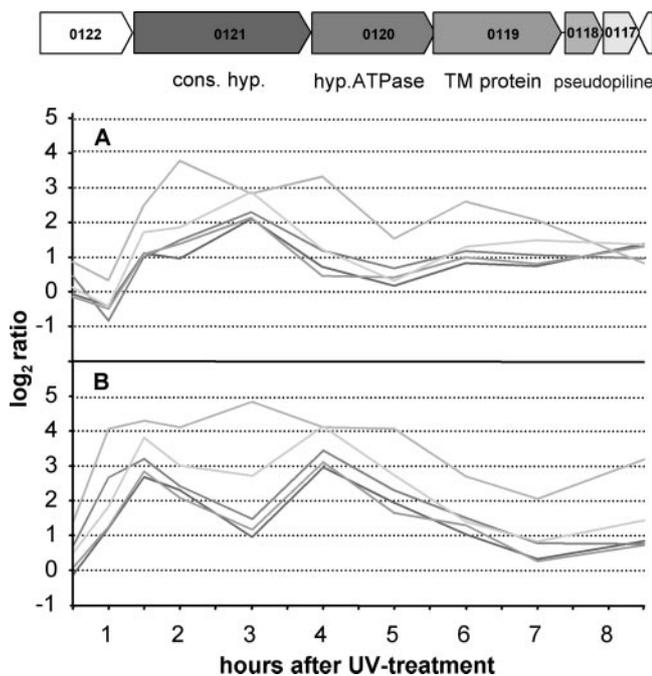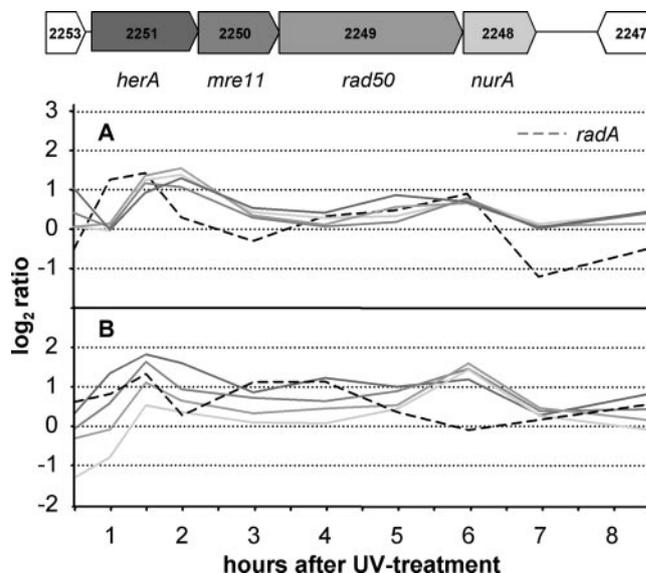

FIG. 7. Expression profile of a strongly UV-induced operon encoding homologs of a putative pilus or secretion system (type II/IV). All five genes show a high induction in both strains PH1 (A) and PH1(SSV1) (B). The genes flanking the operon (SSO0122 and SSO5209) showed no effect after UV light exposure (not shown). Predicted gene functions are based on a bioinformatics analysis (Table 2).

photoreversal and base excision repair, were found to be significantly induced upon UV light exposure. A few data points of genes from the NER system reached relative ratios above twofold (i.e., $\log_2 > 1$), but since they followed the temporal pattern of the general cell cycle-dependent response, we assume that this is not an indication for a specific transcriptional reaction to UV damage but rather reflects a basic and partly synchronized activity of highly transcribed genes. Genes of operon 5 (Table 1, O5) encoding the HerA, Mre11, Rad50, and NurA homologs of *Sulfolobus* showed a moderate (two- to threefold) UV-dependent transcriptional up-regulation (Fig. 8). These factors are supposed to be involved in recombinational repair (6, 21). Other genes involved in recombination processes, like the *radA* gene (SSO0250), the Holliday junction resolvases (SSO0575 and SSO1176), or integrase (SSO0375), however, did not show a UV-dependent expression pattern (Fig. 8, *radA*). We found induction of a RecB-like nuclease (SSO0001) that could play a role in homologous recombination and recombinational DNA repair. Like bcp-2 (SSO2121), it may react due to oxidative stress damage (49).

Among the three identified type B polymerases of *S. solfataricus*, only polymerase II was found to be significantly induced (see Fig. S4III in the supplemental material). This B-type polymerase is encoded by three cotranscribed genes (SSO1459, SSO1458, and SSO8124) that are proposed to generate a full-length DNA polymerase by programmed frameshifting (GenBank accession number AAK41686), as B-family type polymerases usually contain only one polypeptide chain. However, the same triple gene arrangement is found in the

genomes of *Sulfolobus tokodaii* and *Sulfolobus acidocaldarius*. From its transcriptional pattern, we propose that this polymerase should be involved in DNA repair/replication after UV damage. A reaction of the translesion repair polymerase (*dpo4*) was only seen in the uninfected culture, where a significant up-regulation from 4 h to 5 h was observed.

DISCUSSION

When discussing the data of this study in the light of other investigations, it is important to note that the UV dose of 75 J/m^2 we applied was lower than that used in an earlier study of *Sulfolobus solfataricus* and many other bacteria (200 J/m^2) (42) but similar to that used by McCready et al. (30) (30 to 70 J/m^2) for genome-wide transcription studies in *Halobacterium* sp. strain NRC-I. Our survival rates of 10 to 40% for the *S. solfataricus* strain devoid of SSV1 and ~10% for the lysogenic strain are comparable to those found for *S. acidocaldarius* under similar conditions (47) but are considerably lower than those of *Halobacterium* sp. strain NRC-I, which showed over 80% survival after exposure to 70 J/m^2 (30).

The fact that we used two strains (a lysogen and a wild-type nonlysogen) that reacted with almost identical gene sets on the transcriptional level but in a slightly time-shifted manner proved helpful for dissecting the UV-dependent response in *Sulfolobus*. In particular, this helped in distinguishing UV-dependent genes from a large number of highly transcribed, but not UV-induced, genes that appeared significant at certain time points, possibly because of a slight alteration of the cell cycle distribution of the population after UV treatment (Fig. 5). Another aid in dissecting UV-dependent genes was the relatively long time period over which we did the transcriptional analysis (8 to 12 h) and the relatively large number of sampling points.

From the experiments presented here, we can discern three outcomes from UV light-induced damage in *Sulfolobus*.

(i) Growth inhibition, cell death, and cell cycle perturbation. From ca. 1.5 to 2 h after UV treatment, the optical density of the UV-damaged *S. solfataricus* culture decreased over 5 h, reflecting growth retardation of damaged cells and/or the effect of cell death (Fig. 1). We also noted a modest accumulation of cells with a single copy of the chromosome (Fig. 3). This presumably reflects the accumulation of cells that fail to progress into the S phase of the cell cycle. It is possible that this could represent a checkpoint-like response in *Sulfolobus*. However, in light of the persistence of this minority population over the 8.5-h time course and the high levels of mortality caused by UV treatment, it is perhaps more likely that this reflects an increased sensitivity of G$_1$- and early-S-phase cells to UV-induced damage.

With regard to the lack of strong cell cycle responses, it is interesting that we observed clear modulation of the levels of the Cdc6 transcripts. Previous work revealed that treatment of *S. acidocaldarius* with acetic acid perturbed the cell cycle, leading to an accumulation of cells in the G$_2$ phase (38). This was associated with the presence of high levels of Cdc6-2 and almost undetectable levels of Cdc6-1 and Cdc6-3 proteins. Comparing our data set with that of Lundgren and Bernander (25), who investigated cell cycle-dependent transcriptional responses, we found more indications for cell cycle disturbance

after UV treatment, since 18 of our 22 genes that were significantly down-regulated have been classified as being transcribed and up-regulated in a cell cycle-dependent manner ("cyclic") by Lundgren and Bernander (25). Nevertheless, the UV-dependent transcriptional response is clearly distinguishable from the genes identified by Lundgren and Bernander (25), as only four of the up-regulated genes were also found to be cell cycle dependent (*cdc6-2*, *dpoII*, SSO0152, and SSO1823).

Perhaps the most obvious effect observed in the flow cytometry is the appearance of cells with greater than 2N content at late time points. This could be due either to additional rounds of replication occurring inappropriately in G$_2$ cells, to a lack of cell division after mitosis or, as discussed below, to uptake of DNA from other cells during conjugation processes.

(ii) Formation of double-strand breaks and induction of the recombinational repair system. Similar to the results of transcriptome studies in halobacteria (3, 30), we did not find any indication of a concerted UV-dependent regulation, as would be expected in an SOS-like response, nor did we find a significant induction of the repair genes that are involved in direct DNA damage removal, for example, photolyase or components of the putative nucleotide excision repair system. Most probably, these systems are constantly present for instantaneous reaction to DNA damage and therefore do not react dramatically on a transcriptional level. Alternatively, some factors might be posttranslationally modified for activation and therefore would not appear in a transcriptome analysis. While Salerno et al. (42) described some induction for the NER system (after a UV dose of 200 J/m^2), these genes followed the pattern of constitutive, but highly transcribed, genes in our study. While *radA* was induced in *Halobacterium* after a low UV dose, we did not see a significant induction in *Sulfolobus*, confirming earlier results for this organism (43). Interestingly, we saw a relatively weak, but UV-dependent, response of genes from the putative recombinational repair system of *Sulfolobus*, the Mre11 operon, which can also be involved in the repair of double-strand breaks. These results inspired us to analyze the occurrence of double-strand breaks in *Sulfolobus* upon UV treatment. We observed DSB between 2 and 8 h after UV treatment and hypothesize that the unrepaired fraction of CPDs, which were observed from 0 h to 2 h after UV treatment (not shown), leads to the formation of double-strand breaks, which are then processed for recombinational repair, which involves factors of the MRE11 complex (21, 22). Furthermore, we observed a considerable accumulation of cells in the S phase after 8.5 h (Fig. 3, flow cytometry data; see also Fig. S1 in the supplemental material), which might represent the fraction of the culture that resumes replication after the double-strand breaks have been repaired (Fig. 4). As early as 30 years ago, the occurrence of double-strand breaks upon UV treatment had been demonstrated for *E. coli* (4). Recently, it was shown using mouse skin cells that unrepaired CPDs provoke an accumulation of single- and double-strand breaks during DNA replication, which represents a major cause of UV-mediated cytotoxicity (10). Furthermore, CPDs, rather than other DNA lesions or damaged macromolecules, represented the principal mediator of the cellular transcription response to UV (10). The most prominent repair pathways that were induced by CPDs were associated with DNA double-strand

break signaling and repair, including also Mre11a and Rad50, the two eukaryotic homologs of the genes found in the Mre11 operon of *Sulfolobus* (10).

(iii) Formation of cell-to-cell contacts: an indication for conjugation? The strong induction of a type II/IV system of secretion or pilus formation (Table 2) with genes that potentially encode type IV pilin-like signal peptides (1) inspired us to microscopically investigate if cell aggregates indicative of conjugation were formed. We have observed a reproducible, considerable UV-induced formation of aggregates (Fig. 2) as well as the formation of pili (not shown). At least 90% of the cells were found in aggregates, particularly between 3 and 6 h after treatment (not all of them are included in the quantitative statistics of Fig. 2 because of the huge size of the aggregates). The cell clumps resemble those observed in plasmid-mediated conjugation (44). This finding strongly supports earlier observations of an enhanced exchange of genetic markers upon UV treatment (17, 34, 47, 52). Wood et al. performed experiments with strains that were mutated in the *pyrD* or *pyrB* genes, which are involved in de novo uracil formation. The exposure of 70 J/m^2 seemed to yield the highest rate of exchange (52), which is similar to the UV dose under which we found the most aggregates (75 J/m^2).

In light of these observations, we propose that besides well-known DNA repair mechanisms, *Sulfolobus* might use conjugational DNA exchange and subsequent homologous recombination to repair its DNA, since *Sulfolobus* (17, 44), like *Halobacterium* (31, 40), seems to be quite active in conjugation.

Conclusion. In conclusion, our results demonstrate, concurring with other studies, that DNA damage triggers a complex set of events in the cells and that these events involve many different biological processes. Besides direct damage removal, homologous recombination—and perhaps conjugation—might play a considerable role in this network. The majority of genes that were most prominently down- or up-regulated in this study are of unknown function and only have orthologs in other *Sulfolobales* or in crenarchaeota, indicating that the UV-dependent and other stress-related responses and repair mechanisms in *Archaea* are highly diverse and very poorly understood.

REFERENCES

1. **Albers, S. V., and A. J. Driessen.** 2005. Analysis of ATPases of putative secretion operons in the thermoacidophilic archaeon Sulfolobus solfataricus. Microbiology **151:**763–773.

2. **Aravind, L., D. R. Walker, and E. V. Koonin.** 1999. Conserved domains in DNA repair proteins and evolution of repair systems. Nucleic Acids Res. **27:**1223–1242.

3. **Baliga, N. S., S. J. Bjork, R. Bonneau, M. Pan, C. Iloanusi, M. C. Kottemann, L. Hood, and J. DiRuggiero.** 2004. Systems level insights into the stress response to UV radiation in the halophilic archaeon Halobacterium NRC-1. Genome Res. **14:**1025–1035.

4. **Bonura, T., and K. C. Smith.** 1975. Enzymatic production of deoxyribonucleic acid double-strand breaks after ultraviolet irradiation of *Escherichia coli* K-12. J. Bacteriol. **121:**511–517.

5. **Chirgwin, J. M., A. E. Przybyla, R. J. MacDonald, and W. J. Rutter.** 1979. Isolation of biologically active ribonucleic acid from sources enriched in ribonuclease. Biochemistry **18:**5294–5299.

6. **Constantinesco, F., P. Forterre, E. V. Koonin, L. Aravind, and C. Elie.** 2004. A bipolar DNA helicase gene, herA, clusters with rad50, mre11 and nurA genes in thermophilic archaea. Nucleic Acids Res. **32:**1439–1447.

7. **Crowley, D. J., I. Boubriak, B. R. Berquist, M. Clark, E. Richard, L. Sullivan, S. Dassarma, and S. McCready.** 2006. The uvrA, uvrB and uvrC genes are required for repair of ultraviolet light induced DNA photoproducts in Halobacterium sp. NRC-1. Saline Systems **2:**11.

8. **Dorazi, R., D. Gotz, S. Munro, R. Bernander, and M. F. White.** 2007. Equal rates of repair of DNA photoproducts in transcribed and non-transcribed strands in Sulfolobus solfataricus. Mol. Microbiol. **63:**521–529.

9. **Frols, S., P. M. Gordon, M. A. Panlilio, C. Schleper, and C. W. Sensen.** 2007. Elucidating the transcription cycle of the UV-inducible hyperthermophilic archaeal virus SSV1 by DNA microarrays. Virology **356:**48–59.

10. **Garinis, G. A., J. R. Mitchell, M. J. Moorhouse, K. Hanada, H. de Waard, D. Vandeputte, J. Jans, K. Brand, M. Smid, P. J. van der Spek, J. H. Hoeijmakers, R. Kanaar, and G. T. van der Horst.** 2005. Transcriptome analysis reveals cyclobutane pyrimidine dimers as a major source of UV-induced DNA breaks. EMBO J. **24:**3952–3962.

11. **Garrett, R. A., and H.-P. Klenk.** 2006. Archaea: evolution, physiology and molecular biology. Blackwell Publishing Professional, Malden, MA.

12. **Grogan, D. W.** 1989. Phenotypic characterization of the archaebacterial genus *Sulfolobus*: comparison of five wild-type strains. J. Bacteriol. **171:**6710–6719.

13. **Grogan, D. W.** 2004. Stability and repair of DNA in hyperthermophilic Archaea. Curr. Issues Mol. Biol. **6:**137–144.

14. **Grogan, D. W.** 2000. The question of DNA repair in hyperthermophilic archaea. Trends Microbiol. **8:**180–185.

15. **Grogan, D. W., G. T. Carver, and J. W. Drake.** 2001. Genetic fidelity under harsh conditions: analysis of spontaneous mutation in the thermoacidophilic archaeon Sulfolobus acidocaldarius. Proc. Natl. Acad. Sci. USA **98:**7928–7933.

16. **Haber, J. E.** 2006. Chromosome breakage and repair. Genetics **173:**1181–1185.

17. **Hansen, J. E., A. C. Dill, and D. W. Grogan.** 2005. Conjugational genetic exchange in the hyperthermophilic archaeon *Sulfolobus acidocaldarius*: intragenic recombination with minimal dependence on marker separation. J. Bacteriol. **187:**805–809.

18. **Hanzelmann, P., and H. Schindelin.** 2006. Binding of 5′-GTP to the C-terminal FeS cluster of the radical S-adenosylmethionine enzyme MoaA provides insights into its mechanism. Proc. Natl. Acad. Sci. USA **103:**6829–6834.

19. **Hayashi, M., T. Fukuzawa, H. Sorimachi, and T. Maeda.** 2005. Constitutive activation of the pH-responsive Rim101 pathway in yeast mutants defective in late steps of the MVB/ESCRT pathway. Mol. Cell. Biol. **25:**9478–9490.

20. **Hjort, K., and R. Bernander.** 1999. Changes in cell size and DNA content in *Sulfolobus* cultures during dilution and temperature shift experiments. J. Bacteriol. **181:**5669–5675.

21. **Hopfner, K. P., C. D. Putnam, and J. A. Tainer.** 2002. DNA double-strand break repair from head to tail. Curr. Opin. Struct. Biol. **12:**115–122.

22. **Jazayeri, A., J. Falck, C. Lukas, J. Bartek, G. C. Smith, J. Lukas, and S. P. Jackson.** 2006. ATM- and cell cycle-dependent regulation of ATR in response to DNA double-strand breaks. Nat. Cell Biol. **8:**37–45.

23. **Kelman, Z., and M. F. White.** 2005. Archaeal DNA replication and repair. Curr. Opin. Microbiol. **8:**669–676.

24. **Kulaeva, O. I., E. V. Koonin, J. P. McDonald, S. K. Randall, N. Rabinovich, J. F. Connaughton, A. S. Levine, and R. Woodgate.** 1996. Identification of a DinB/UmuC homolog in the archeon Sulfolobus solfataricus. Mutat. Res. **357:**245–253.

25. **Lundgren, M., and R. Bernander.** 2007. Genome-wide transcription map of an archaeal cell cycle. Proc. Natl. Acad. Sci. USA **104:**2939–2944.

26. **Makarova, K. S., L. Aravind, N. V. Grishin, I. B. Rogozin, and E. V. Koonin.** 2002. A DNA repair system specific for thermophilic Archaea and bacteria predicted by genomic context analysis. Nucleic Acids Res. **30:**482–496.

27. **Martin, A., S. Yeats, D. Janekovic, W. D. Reiter, W. Aicher, and W. Zillig.** 1984. SAV 1, a temperate U.V.-inducible DNA virus-like particle from the archaebacterium Sulfolobus acidocaldarius isolate B12. EMBO J. **3:**2165–2168.

28. **Martusewitsch, E., C. W. Sensen, and C. Schleper.** 2000. High spontaneous

mutation rate in the hyperthermophilic archaeon *Sulfolobus solfataricus* is mediated by transposable elements. J. Bacteriol. **182:**2574–2581.

29. **McCready, S., and L. Marcello.** 2003. Repair of UV damage in Halobacterium salinarum. Biochem. Soc. Trans. **31:**694–698.

30. **McCready, S., J. A. Muller, I. Boubriak, B. R. Berquist, W. L. Ng, and S. Dassarma.** 2005. UV irradiation induces homologous recombination genes in the model archaeon, Halobacterium sp. NRC-1. Saline Systems **1:**3.

31. **Papke, R. T., J. E. Koenig, F. Rodriguez-Valera, and W. F. Doolittle.** 2004. Frequent recombination in a saltern population of Halorubrum. Science **306:**1928–1929.

32. **Raychaudhuri, S., P. Karmakar, D. Choudhary, A. Sarma, and A. R. Thakur.** 2003. Effect of heavy ion irradiation on DNA DSB repair in Methanosarcina barkeri. Anaerobe **9:**15–21.

33. **Reilly, M. S., and D. W. Grogan.** 2002. Biological effects of DNA damage in the hyperthermophilic archaeon Sulfolobus acidocaldarius. FEMS Microbiol. Lett. **208:**29–34.

34. **Reilly, M. S., and D. W. Grogan.** 2001. Characterization of intragenic recombination in a hyperthermophilic archaeon via conjugational DNA exchange. J. Bacteriol. **183:**2943–2946.

35. **Reiter, W. D., P. Palm, and W. Zillig.** 1988. Analysis of transcription in the archaebacterium Sulfolobus indicates that archaebacterial promoters are homologous to eukaryotic pol II promoters. Nucleic Acids Res. **16:**1–19.

36. **Robb, F. T., D. L. Maeder, J. R. Brown, J. DiRuggiero, M. D. Stump, R. K. Yeh, R. B. Weiss, and D. M. Dunn.** 2001. Genomic sequence of hyperthermophile, Pyrococcus furiosus: implications for physiology and enzymology. Methods Enzymol. **330:**134–157.

37. **Robinson, N. P., K. A. Blood, S. A. McCallum, P. A. Edwards, and S. D. Bell.** 2007. Sister chromatid junctions in the hyperthermophilic archaeon Sulfolobus solfataricus. EMBO J. **26:**816–824.

38. **Robinson, N. P., I. Dionne, M. Lundgren, V. L. Marsh, R. Bernander, and S. D. Bell.** 2004. Identification of two origins of replication in the single chromosome of the archaeon Sulfolobus solfataricus. Cell **116:**25–38.

39. **Romano, V., A. Napoli, V. Salerno, A. Valenti, M. Rossi, and M. Ciaramella.** 2007. Lack of strand-specific repair of UV-induced DNA lesions in three genes of the archaeon Sulfolobus solfataricus. J. Mol. Biol. **365:**921–929.

40. **Rosenshine, I., R. Tchelet, and M. Mevarech.** 1989. The mechanism of DNA transfer in the mating system of an archaebacterium. Science **245:**1387–1389.

41. **Saeed, A. I., V. Sharov, J. White, J. Li, W. Liang, N. Bhagabati, J. Braisted, M. Klapa, T. Currier, M. Thiagarajan, A. Sturn, M. Snuffin, A. Rezantsev,** D. Popov, A. Ryltsov, E. Kostukovich, I. Borisovsky, Z. Liu, A. Vinsavich, V. Trush, and J. Quackenbush. 2003. TM4: a free, open-source system for microarray data management and analysis. BioTechniques **34:**374–378.

42. **Salerno, V., A. Napoli, M. F. White, M. Rossi, and M. Ciaramella.** 2003. Transcriptional response to DNA damage in the archaeon Sulfolobus solfataricus. Nucleic Acids Res. **31:**6127–6138.

43. **Sandler, S. J., L. H. Satin, H. S. Samra, and A. J. Clark.** 1996. recA-like genes from three archaean species with putative protein products similar to Rad51 and Dmc1 proteins of the yeast Saccharomyces cerevisiae. Nucleic Acids Res. **24:**2125–2132.

44. **Schleper, C., I. Holz, D. Janekovic, J. Murphy, and W. Zillig.** 1995. A multicopy plasmid of the extremely thermophilic archaeon *Sulfolobus* effects its transfer to recipients by mating. J. Bacteriol. **177:**4417–4426.

45. **Schleper, C., K. Kubo, and W. Zillig.** 1992. The particle SSV1 from the extremely thermophilic archaeon Sulfolobus is a virus: demonstration of infectivity and of transfection with viral DNA. Proc. Natl. Acad. Sci. USA **89:**7645–7649.

46. **Schleper, C., R. Roder, T. Singer, and W. Zillig.** 1994. An insertion element of the extremely thermophilic archaeon Sulfolobus solfataricus transposes into the endogenous beta-galactosidase gene. Mol. Gen. Genet. **243:**91–96.

47. **Schmidt, K. J., K. E. Beck, and D. W. Grogan.** 1999. UV stimulation of chromosomal marker exchange in Sulfolobus acidocaldarius: implications for DNA repair, conjugation and homologous recombination at extremely high temperatures. Genetics **152:**1407–1415.

48. **Stetter, K.** 2006. History of discovery of the first hyperthermophiles. Extremophiles **10:**357–362.

49. **Stohl, E. A., and H. S. Seifert.** 2006. *Neisseria gonorrhoeae* DNA recombination and repair enzymes protect against oxidative damage caused by hydrogen peroxide. J. Bacteriol. **188:**7645–7651.

50. **Turinsky, A. L., A. C. Ah-Seng, P. M. Gordon, J. N. Stromer, M. L. Taschuk, E. W. Xu, and C. W. Sensen.** 2005. Bioinformatics visualization and integration with open standards: the Bluejay genomic browser. In Silico Biol. **5:**187–198.

51. **Williams, E., T. M. Lowe, J. Savas, and J. Diruggiero.** 2007. Microarray analysis of the hyperthermophilic archaeon Pyrococcus furiosus exposed to gamma irradiation. Extremophiles **11:**19–29.

52. **Wood, E. R., F. Ghane, and D. W. Grogan.** 1997. Genetic responses of the thermophilic archaeon *Sulfolobus acidocaldarius* to short-wavelength UV light. J. Bacteriol. **179:**5693–5698.